Strange attractors in a crossover current instability in n-type GaAs: Quality test of $f(\alpha)$ spectrum

Kazunori Aoki and Takayasu Kondo
Department of Electrical Engineering, Faculty of Engineering, Kobe University, Rokkodai, Nada, Kobe 657, Japan
(Received 12 August 1991)

The multifractal nature of the strange attractors observed in a crossover current instability in n-type GaAs has been investigated, mainly focusing on the noise-floor effects. By comparing with a model simulation, quality of the $f(\alpha)$ spectrum has been tested for the strange attractors resulting from period-doubling cascade. It has been found that the model simulation for the crossover instability explains satisfactorily the observed $f(\alpha)$ spectrum under the noise floor.

In nonlinear resistive semiconductors, multiplicative currents caused by the negative differential resistance show frequently chaotic behaviors under different regimes of the electronic instabilities.[1-4] An advantage of studying chaos in semiconductors is due to the fact that nonlinear carrier transport theory is fundamentally well known, especially for the impact ionization process of the frozen-out impurities at low temperature, so that one can construct the nonlinear-dynamical model(s) to criticize the chaotic behaviors observed in the experiments.[1-4] In a model simulation for the driven chaos,[1,2] for instance, rich structures of the bifurcations and chaos have been presented to explain the experimental results.[1] So, one can test crucially the underlying multifractal nature of chaos observed in an experiment by consulting the constructed model. In this Brief Report, we shall study strange attractors observed in a crossover current instability[4] related to low-temperature impurity breakdown in a semiconductor GaAs. We will discuss the multifractal nature of chaos observed just after the period-doubling cascade and the subsequent boundary crisis. The latter half of this paper is concerned with the model simulation in order to discuss the multifractal aspects observed under the noise floor of the experimental system. Briefly, the multifractal nature in the present system is compared with that observed in a driven-chaos system.[1,2]

The experimental procedure has been described in detail previously[4] for the observation of the crossover instability. The sample is a high-purity n-type GaAs with the donor concentration of $\sim 2\times 10^{14}/\mathrm{cm}^3$, which has been grown epitaxially on a semi-insulating substrate. The thickness of the epilayer was about 12 μm. The surface area dimension of the sample was typically $\sim 1.5\times 4$ mm^2. Planar-type Ohmic contacts were formed on the broad crystal surface [Fig. 1(a)]. By immersing the sample into liquid helium of 4.2 K, one can observe a typical hysteresis of the current-voltage characteristics [Fig. 1(b)], which is highly stable in the absence of the magnetic field. By applying a longitudinal magnetic field with the intensity B, the holding voltage V_h shifts toward higher voltages, followed by the narrowing of the hysteresis. Above a critical field of $B_c \sim 40$ mT, the holding voltage exceeds the breakdown voltage V_b, resulting in the crossover current instability[4] [Fig. 1(c)]. The self-oscillation of the current is apparently caused by the repeating cycle of a generation-annihilation process of the current filament, where the destabilization of the filament is explained by the inhomogeneous magnetoresistance effects which act upon the filament boundaries.[4] It is noticed that the local magnetoresistance can be expected for an inhomogeneous spatial pattern as in Fig. 1(a). Images of the inhomogeneous spatial patterns for the samples of the same origin as used in the present study have been actually measured by using low-temperature scanning electron microscopy.[5] In Fig. 1(c), the Hopf-bifurcation route to chaos is observed in the prebreakdown regime[6] (region A), while period-doubling bifurcation can be found in the postbreakdown regime (region B), as discussed below. Between two regimes, the large-amplitude current oscillations exhibit fully developed electronic turbulence.

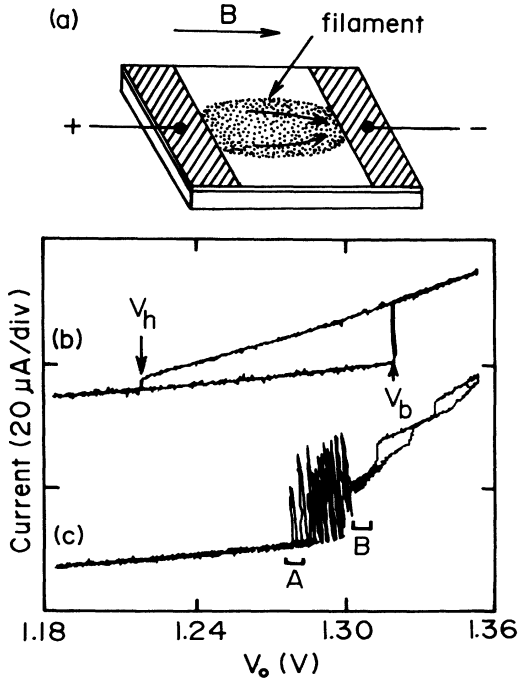

FIG. 1. (a) Sample geometry, and (b), (c) I-V curves under $B=0$ T and $B=65$ mT, respectively, where V_0 is the applied voltage. The load resistance used is $R_L=500\ \Omega$.

Figure 2 shows a series of the current wave forms (left column) and the corresponding Fourier power spectra (right column) observed as a function of B, where $V_0=2.339$ V.[6] The multifractal nature of chaos is analyzed for the time series in Figs. 2(e) and 2(g), resulting from period-doubling bifurcation. In Fig. 2, period 1 bifurcates to period 2 [Fig. 2(c)] with $B \gtrsim 69$ mT. Due to the noise floor embedded in the system, period 4 was not clearly resolved within an extremely narrow range of the control parameter ($69.9 \lesssim B \lesssim 79.8$ mT). With $B \gtrsim 84.6$ mT, the Fourier power spectrum shows broadening of the subharmonic frequency component $f_0/2$ (denoted by an asterisk in Fig. 2) as well as an increase of the background noise level [approximately by 20 dB in Figs. 2(h) and 2(j)].

The Poincaré section analysis of the phase portraits for Figs. 2(e) and 2(g) are shown in Figs. 3(a) and 3(b), which indicates that the period-2-like attractor in Fig. 2(e) undergoes a boundary crisis[7,8] by increasing the magnetic-field intensity from 79.8 to 84.6 mT [Fig. 2(g)] or 85.3 mT [Fig. 2(i)] [the intermittent behaviors are noted by bars in the current wave forms of Figs. 2(g) and 2(i)]. In Fig. 3(b), separatrices (stable orbits of unstable manifold) are speculated by a dashed line.

The singularity spectra[9] $f(\alpha)$ are evaluated by following a procedure by Mino, Yamazaki, and Nakamura[10] in an experiment of parallel-pumped spin-wave instability. The strange attractors are constructed in five-dimensional phase space by using the time lagging method. In order to get the so-called generalized dimension D_q, we first

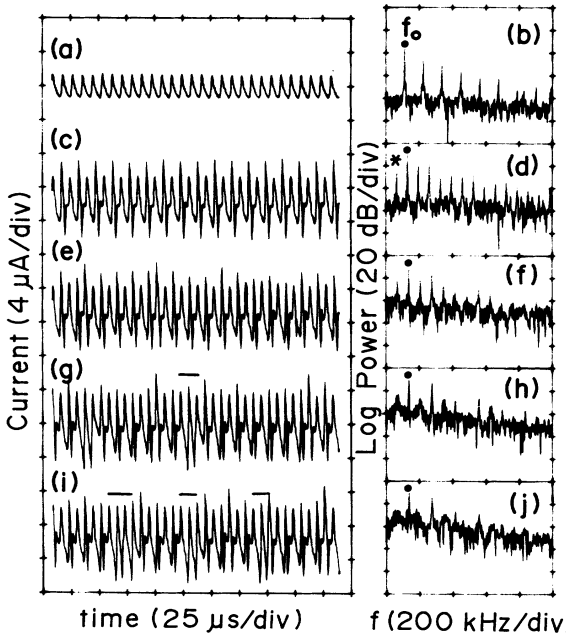

FIG. 2. A series of the current wave forms (left column) and the Fourier power spectra (right column) as a function of B, where $B=59$ mT in (a) and (b), $B=69.9$ mT in (c) and (d), $B=79.8$ mT in (e) and (f), $B=84.6$ mT in (g) and (h), and $B=85.3$ mT in (i) and (j). The natural frequencies f_0 are (b) 113 kHz, (d) 131 kHz, (f) 139 kHz, and (j) 141 kHz. $R_L=10$ kΩ.

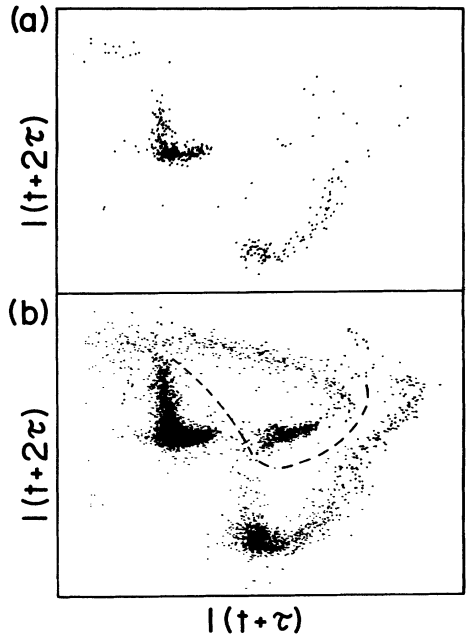

FIG. 3. Poincaré sections of the three-dimensional phase portraits: (a) $B=79.8$ mT and (b) $B=84.6$ mT. The time lag is chosen to be $\tau=1.5$ μs.

calculate the partition function $\Gamma(q,l)=(1/n)\times\sum_i P_i(l)^{q-1}$, where $P_i(l)$ is the probability which is obtained by counting the number of data points within the ith hypersphere of radius l ($i=1,2,\ldots,n$) and dividing it by the total number N of data points of the attractor.[10] The total number of the data points used was $N=6000$ for the attractor in Fig. 3(a) and $N=30000$ for the attractor in Fig. 3(b). The hyperspheres were randomly chosen with the total number of $n=1000$ for the attractor in Fig. 3(a) and $n=3000$ for the attractor in Fig. 3(b). From the scaling law $\Gamma(q,l)\sim l^{(q-1)D_q}$, the D_q curve is obtained and finally the $f(\alpha)$ spectrum is calculated from the Legendre transformation.[9] The aim is to clarify the noise effect on the $f(\alpha)$ spectrum. As has been described in the pioneering works by Halsey *et al.*,[9] local singularities of different strengths α are distributed on the interwoven sets of the dimensionality $f(\alpha)$, where densely (sparsely) distributed fractalities are related to $\Gamma(q,l)$ or $P_i(l)^{q-1}$ for large positive (negative) q values, respectively. When the external noise is added in the system, it affects seriously the right-half side of $f(\alpha)$. Very frequently, one cannot obtain the right-half side[11] because sparsely distributed regions of the attractor become more sparse by the external noise and it happens that the scaling law for $q<0$ is broken by the most rarified hyperspheres which include only a few data points inside the small radius l. By filtering (rejecting) such rarified hyperspheres, one can recover the right-half side of $f(\alpha)$, where the scaling in $\Gamma(q,l)$ can be taken typically for $q \gtrsim -6$ and with the precision approximately up to the scale $l\sim 2^{-4}$ (we term the numerical procedure a filtering method).

Figures 4(a) and 4(b) show the $f(\alpha)$ spectra for the

period-2-like attractor ($B=79.8$ mT) in 4(a) and for the extended attractor after the crisis ($B=84.6$ mT) in 4(b), respectively, where the solid circles are the experimental results obtained by the filtering method (the solid lines are those of the model simulation, as discussed below). The capacity dimensions are $D_0 \sim 1.69 \pm 0.1$ in Fig. 4(a), and $D_0 \sim 2.24 \pm 0.1$ in Fig. 4(b), respectively. With further increase of B, the $f(\alpha)$ shows the growth of the higher-dimensional attractor (e.g., $D_0 \sim 2.49$ with $B=115.3$ mT). Apparently, the experimental results in Figs. 4(a) and 4(b) exhibit much broader spectra than those in the model simulation. The large discrepancies are attributed to the noise effects, which will be discussed later returning back to Figs. 4(c) and 4(d).

Before discussing the noise effects, we briefly describe the model simulation.[4] The order parameters are the electron's mean kinetic energy ε, magnetoresistance factor h, electron density n, and electric field E. A couple of the rate equations are given by

$$\dot{\varepsilon} = -(\varepsilon - \varepsilon_L)/\tau(\varepsilon) + e\mu_B E^2, \quad \mu_B = \mu h \ , \tag{1}$$

$$\dot{h} = -\gamma(h - h_0) \ , \tag{2}$$

$$\dot{n} = n(N_D - N_A - n)A_I + (N_D - N_A - n)A_T - n(n + N_A)B_T \ , \tag{3}$$

$$\dot{E} = -\gamma_d[E - E_0 + cne\mu_B E + \xi(t)] \ , \tag{4}$$

where ε_L denotes the thermal energy, $\tau(\varepsilon) \propto \varepsilon^{-1/2}$ the energy relaxation time, μ_B the electron mobility under the magnetic field, μ the zero-field electron mobility, h_0 the magnetoresistance factor under the steady state,[4] A_I the impact-ionization coefficient, A_T (B_T) the thermal ionization (recombination) coefficient, γ and γ_d are the damping constants, N_D (N_A) the donor (acceptor) concentration, $\xi(t)$ the external noise if required, E_0 the applied electric field, c is a positive constant, and the overdots in (1)–(4) denote the time derivatives, respectively. In a few words, an important aspect for the crossover instability in (1)–(4) is the following.[4] The energy gain of impact-ionized carriers by an electric field is given by $e\mu_B E^2$. Under the longitudinal magnetic field, the holding field E_h' shifts toward higher fields by the relation $E_h' = \sqrt{\mu/\mu_B} E_h$ ($e\mu_B E_h'^2 = e\mu E_h^2$, E_h is the holding field under $B=0$), while the breakdown field E_b is kept constant.[4] Above a critical value of $B_c = 0.143$ T, E_h' exceeds E_b and the crossover current instability sets in (for detailed descriptions, see Ref. 4).

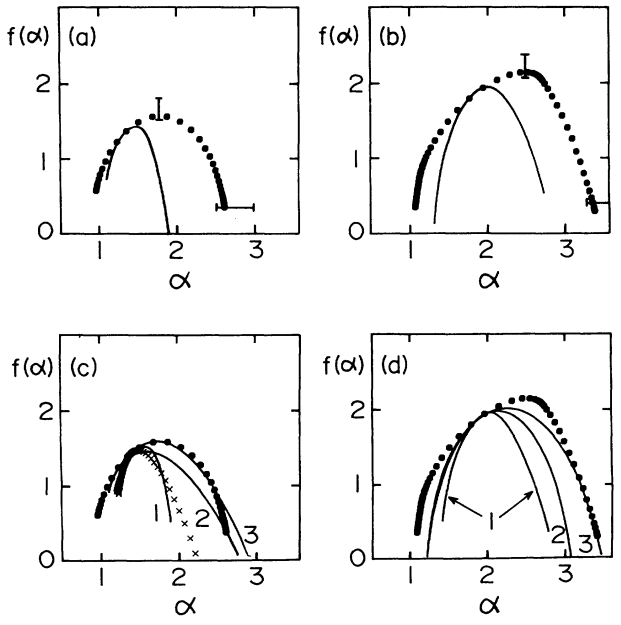

FIG. 4. Experimental $f(\alpha)$ spectra (solid circles): (a) $B=79.8$ mT and (b) $B=84.6$ mT. Solid lines are by the model simulations: (a) $B=154.921$ mT and (b) $B=155$ mT. Corresponding to (a) and (b), broadening effects of the simulated $f(\alpha)$ spectra are shown in (c) and (d), respectively, as a function of noise level: (1) $\sigma = 2.886 \times 10^{-5}$, (2) $\sigma = 8.66 \times 10^{-5}$, and (3) $\sigma = 1.442 \times 10^{-4}$.

By using the same parameter values as those used in Ref. 4 and with $\xi(t)=0$, we show the bifurcation diagram as a function of B in Fig. 5, where peak values ν_p of the electron density [$\nu = n/(N_D - N_A)$] are plotted in the ordinate for each parameter value of B. Figure 5 shows typically the period-doubling bifurcation in the post-breakdown regime [cf. region B in Fig. 1(c)]. For $B \gtrsim 0.154\,94$ T, there appears suddenly a boundary crisis[7,8] or chaos-chaos transition, as indicated by an arrow. The bifurcation regime explains very well the experimental results in Fig. 2. It is remarked that the $f(\alpha)$ spectra in Figs. 4(a) and 4(b) (solid lines) were calculated, respectively, for the period-2-like attractor at $B=0.154\,921$ T and the fully extended attractor at $B=0.155$ T. The solid line in Fig. 4(a) is found to be relatively similar to (but slightly broader than) that of the Feigenbaum attractor,[9] by subtracting the trivial dimensionality one ($D_0=0.52$, $D_\infty=0.25$, $D_{-\infty}=0.8$).

Returning to the noise effects on the $f(\alpha)$ spectrum, the random fluctuating force is added in (4), where $\langle \xi(t) \rangle = 0$ and the variance $\sigma^2 = \langle \xi^2(t) \rangle$. In Figs. 4(c) and 4(d), the simulated $f(\alpha)$ spectra are shown by solid

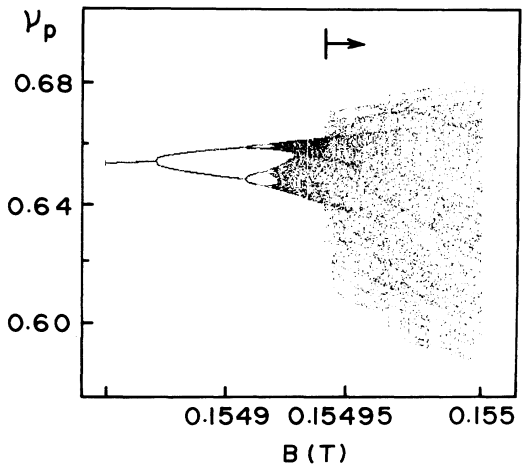

FIG. 5. Bifurcation diagram as a function of B in the model simulation.

lines labeled by 1–3 for three different noise levels: (1) $\sigma=2.886\times10^{-5}$, (2) $\sigma=8.66\times10^{-5}$, and (3) $\sigma=1.442\times10^{-4}$ (the filtering method has been used for $\sigma>0$). By increasing the noise level, it is found that the singularity spectrum broadens especially toward larger singularity strengths, while the capacity dimension D_0 is slightly increased, as recognized in Figs. 4(c) and 4(d). The experimental results (solid circles) are best fitted to the simulated result with $\sigma=1.442\times10^{-4}$ (curve 3). For reference, crosses in Fig. 4(c) show the $f(\alpha)$ spectrum obtained typically for the periodically driven chaos,[1,2] which has resulted from the period-doubling cascade (bifurcated from period 4). The spectrum is much narrower than that observed in the crossover instability (present case) and relatively close to the spectrum of the Feigenbaum attractor.[9] Both of the results [crosses and solid circles in Fig. 4(c)] have been obtained with the same quality of the minimal noise levels in the experimental systems. Therefore it is found that the external noise influences the multifractal natures of the strange attractors in different manners depending upon the types of the spatially extended instabilities of the current filament.[12]

In conclusion, we have criticized the quality of the strange attractors observed in a crossover instability in n-type GaAs. The model simulation explains very well the observed results by taking into account the external noise. The filtering method has been exemplified to be a conventional and powerful method to evaluate the $f(\alpha)$ spectrum in a system with relatively small signals under the noise floor.

The authors thank K. Yamamoto for valuable discussions. This work was partly supported by a Grant-in-Aid for Scientific Research from the Ministry of Education, Science and Culture.

[1]K. Aoki, K. Yamamoto, and N. Mugibayashi, J. Phys. Soc. Jpn. **57**, 26 (1988).

[2]K. Aoki and K. Yamamoto, Appl. Phys. A **48**, 111 (1989); K. Aoki and N. Mugibayashi, *ibid.* **48**, 161 (1989).

[3]E. G. Gwinn and R. M. Westervelt, Phys. Rev. Lett. **59**, 157 (1987).

[4]K. Aoki, T. Kondo, and T. Watanabe, Solid State Commun. **77**, 91 (1991); for the model simulations, see K. Aoki, *ibid.* **77**, 87 (1991); Phys. Lett. A **152**, 485 (1991).

[5]K. Aoki, U. Rau, J. Peinke, J. Parisi, and R. P. Huebener, J. Phys. Soc. Jpn. **59**, 420 (1990); U. Rau, K. Aoki, J. Peinke, J. Parisi, W. Clauss, and R. P. Huebener, Z. Phys. B **81**, 53 (1990).

[6]For the study of the bifurcation, we used a large value of the load resistance (10 kΩ) and thus large values of V_0, e.g., see K. Aoki, in *Proceedings of the 20th International Conference on the Physics of Semiconductors,* edited by E. M. Anastassakis and J. D. Joannopoulos (World Scientific, Singapore, 1990), p. 2578.

[7]C. Grebogi, E. Ott, and J. A. Yorke, Phys. Rev. Lett. **57**, 1284 (1986).

[8]Y. Aizawa and T. Uezu, Prog. Theor. Phys. **68**, 1864 (1982).

[9]T. C. Halsey, M. H. Jensen, L. P. Kadanoff, I. Procaccia, and B. I. Shraiman, Phys. Rev. A **33**, 1141 (1986).

[10]M. Mino, H. Yamazaki, and K. Nakamura, Phys. Rev. B **40**, 5279 (1989).

[11]R. R. Prasad, C. Meneveau, and K. R. Sreenivasan, Phys. Rev. Lett. **61**, 74 (1988).

[12]Theoretically, the filament boundaries are extremely sensitive to the external perturbations or noise, e.g., see E. Schöll, *Nonequilibrium Phase Transitions in Semiconductors* (Springer-Verlag, Berlin, 1987).

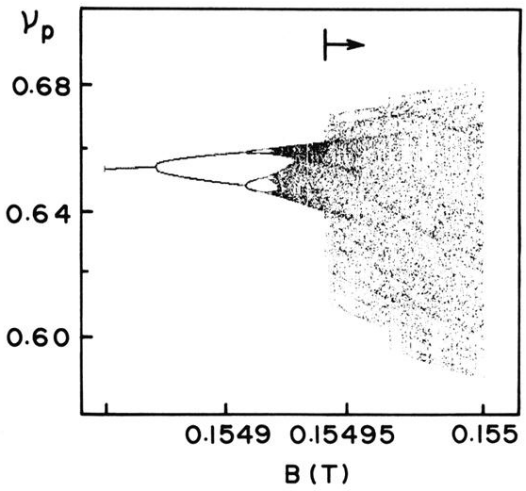

FIG. 5. Bifurcation diagram as a function of B in the model simulation.